

Rhodium-Catalyzed Dehydrocoupling of the Sterically Encumbered Phosphine–Borane Adduct $t\text{Bu}_2\text{PH}\cdot\text{BH}_3$: Synthesis of the Linear Dimers $t\text{Bu}_2\text{PH}-\text{BH}_2-t\text{Bu}_2\text{P}-\text{BH}_3$ and $t\text{Bu}_2\text{PH}-\text{BH}_2-t\text{Bu}_2\text{P}-\text{BH}_2\text{Cl}$

Hendrik Dorn, Emira Vejzovic, Alan J. Lough, and Ian Manners*

Department of Chemistry, University of Toronto, 80 St. George Street, Toronto, Ontario, M5S 3H6, Canada

Received January 17, 2001

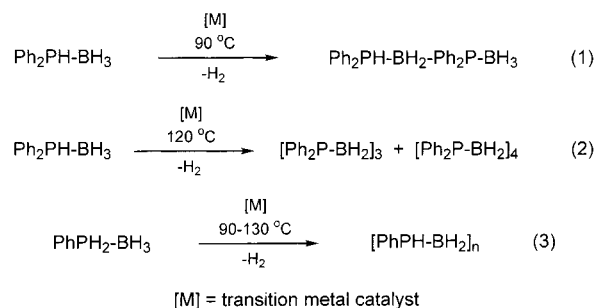
The dehydrocoupling of the sterically hindered phosphine–borane adduct $t\text{Bu}_2\text{PH}\cdot\text{BH}_3$ above 140 °C is catalyzed by the rhodium complexes $[\text{Rh}(1,5\text{-cod})_2][\text{OTf}]$ or $\text{Rh}_6(\text{CO})_{16}$ to give the four-membered chain $t\text{Bu}_2\text{PH}-\text{BH}_2-t\text{Bu}_2\text{P}-\text{BH}_3$ (**1**), which was isolated in 60% yield and characterized by multinuclear NMR spectroscopy, mass spectrometry, and elemental analysis. Thermolysis of **1** in the temperature range 175–180 °C led to partial decomposition and the formation of $t\text{Bu}_2\text{PH}\cdot\text{BH}_3$. When the dehydrocoupling of $t\text{Bu}_2\text{PH}\cdot\text{BH}_3$ was performed in the presence of $[\{\text{Rh}(\mu\text{-Cl})(1,5\text{-cod})\}_2]$ or RhCl_3 hydrate, the chlorinated compound $t\text{Bu}_2\text{PH}-\text{BH}_2-t\text{Bu}_2\text{P}-\text{BH}_2\text{Cl}$ (**2**) was formed which could not be obtained free of **1**. The molecular structures of $t\text{Bu}_2\text{PH}\cdot\text{BH}_3$, $t\text{Bu}_2\text{PH}-\text{BH}_2-t\text{Bu}_2\text{P}-\text{BH}_3$ (**1**), and $t\text{Bu}_2\text{PH}-\text{BH}_2-t\text{Bu}_2\text{P}-\text{BH}_2\text{Cl}$ (**2**) together with **1** were determined by single-crystal X-ray diffraction studies.

Introduction

The development of new and efficient synthetic procedures for the formation of bonds between main group elements is of importance for the construction of inorganic polymer chains and also for the general development of p-block chemistry. In recent years, transition-metal-catalyzed dehydrocoupling routes have been established for the preparation of homonuclear and heteronuclear bonds between main group elements.¹ Species containing Si–Si,^{1,2} Ge–Ge,^{1,3} Sn–Sn,^{1,4} P–P,^{1,5} B–Si,⁶ P–Si,⁷ and O–Si⁸ bonds have received particular attention.

As part of our continuing program to develop novel extended structures based on main group elements, we are currently exploring compounds with four-coordinate phosphorus and boron atoms. Cyclic phosphinoboranes of the general formula $[\text{R}_2\text{P}-\text{BH}_2]_x$ (R = alkyl or aryl, $x = 3$) are well-known as a result of the pioneering work of Burg and Wagner in the 1950s.^{9,10} In contrast, the synthesis of well-characterized linear and polymeric phosphinoboranes represents a relatively unex-

Scheme 1



plored area of research.¹¹ We have recently reported the transition-metal-catalyzed dehydrocoupling of the phosphine–borane adducts $\text{Ph}_2\text{PH}\cdot\text{BH}_3$ and $\text{RPH}_2\cdot\text{BH}_3$ (R = Ph or $i\text{Bu}$) to yield novel linear and cyclic phosphinoboranes, as well as the first high molecular weight polyphosphinoboranes (Scheme 1).^{12–15} For example, dehydrocoupling of $\text{Ph}_2\text{PH}\cdot\text{BH}_3$ at 90 °C in the presence of rhodium complexes such as $[\text{Rh}(1,5\text{-cod})_2][\text{OTf}]$ (cod = cyclooctadiene) or $[\{\text{Rh}(\mu\text{-Cl})(1,5\text{-cod})\}_2]$ was found to result in the quantitative formation of the four-membered chain $\text{Ph}_2\text{PH}-\text{BH}_2-\text{Ph}_2\text{P}-\text{BH}_3$, whereas at more elevated temperatures (120 °C) a mixture of the rings $[\text{Ph}_2\text{P}-\text{BH}_2]_3$ and $[\text{Ph}_2\text{P}-\text{BH}_2]_4$ is formed. In contrast, rhodium-catalyzed dehydrocoupling of the primary phosphine–borane adduct $\text{PhPH}_2\cdot\text{BH}_3$ afforded the high molecular weight poly-

* To whom correspondence should be addressed. E-mail: imanners@alchemy.chem.utoronto.ca.

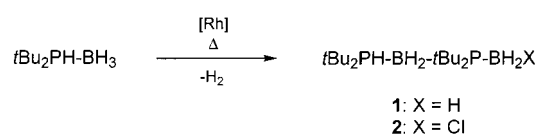
- (1) For a recent review on catalytic dehydrocoupling, see: Gauvin, F.; Harrod, J. F.; Woo, H. G. *Adv. Organomet. Chem.* **1998**, *42*, 363.
- (2) (a) Aitken, C. T.; Harrod, J. F.; Samuel, E. *J. Am. Chem. Soc.* **1986**, *108*, 4059. (b) Tilley, T. D. *Acc. Chem. Res.* **1993**, *26*, 22.
- (3) For catalytic demethanative coupling, see: Katz, S. M.; Reichl, J. A.; Berry, D. H. *J. Am. Chem. Soc.* **1998**, *120*, 9844.
- (4) (a) Imori, T.; Tilley, T. D. *J. Chem. Soc., Chem. Commun.* **1993**, 1607. (b) Imori, T.; Lu, V.; Cai, H.; Tilley, T. D. *J. Am. Chem. Soc.* **1995**, *117*, 9931. (c) Babcock, J. R.; Sita, L. R. *J. Am. Chem. Soc.* **1996**, *118*, 12481.
- (5) Etkin, N.; Fermin, M. C.; Stephan, D. W. *J. Am. Chem. Soc.* **1997**, *119*, 2954.
- (6) Jiang, Q.; Carroll, P. J.; Berry, D. H. *Organometallics* **1993**, *12*, 177.
- (7) Shu, R.; Hao, L.; Harrod, J. F.; Woo, H.-G.; Samuel, E. *J. Am. Chem. Soc.* **1998**, *120*, 12988.
- (8) Zhang, R.; Mark, J. E.; Pinhas, A. R. *Macromolecules* **2000**, *33*, 3508.
- (9) Burg, A. B.; Wagner, R. I. *J. Am. Chem. Soc.* **1953**, *75*, 3872.
- (10) For reviews, see: (a) Parshall, G. W. In *The Chemistry of Boron and its Compounds*; Muetterties, E. L., Ed.; Wiley: New York, 1967; p 617. (b) Haiduc, I. *The Chemistry of Inorganic Ring Systems*; Wiley: New York, 1970; p 349.

- (11) See, for example: (a) Wagner, R. I.; Caserio, F. F. *J. Inorg. Nucl. Chem.* **1959**, *11*, 259. (b) Burg, A. B. *J. Inorg. Nucl. Chem.* **1959**, *11*, 258.
- (12) Dorn, H.; Singh, R. A.; Massey, J. A.; Lough, A. J.; Manners, I. *Angew. Chem., Int. Ed.* **1999**, *38*, 3321.
- (13) Dorn, H.; Singh, R. A.; Massey, J. A.; Nelson, J. M.; Jaska, C. A.; Lough, A. J.; Manners, I. *J. Am. Chem. Soc.* **2000**, *122*, 6669.
- (14) Dorn, H.; Jaska, C. A.; Singh, R. A.; Lough, A. J.; Manners, I. *Chem. Commun.* **2000**, 1041.
- (15) For a recent report of N–B bond formation by catalytic dehydrocoupling, see: Jaska, C. A.; Temple, K.; Lough, A. J.; Manners, I. *Chem. Commun.*, in press.

Table 1. Dehydrocoupling of *t*Bu₂PH·BH₃^a

entry	catalyst	cat. load (mol % Rh)	temp (°C)	time (h)	conversion ^b (%)	products ^b (%)
1	[Rh(1,5-cod) ₂][OTf]	3	140	16	75	1 (70), others (5) ^c
2	none		140	16	0	
3	[Rh(1,5-cod) ₂][OTf]	3	160	3	40	1 (35), others (5) ^c
4	Rh ₆ (CO) ₁₆	3	160	3	60	1 (60)
5	[{Rh(<i>μ</i> -Cl)(1,5-cod)} ₂]	3	160	3	80	1 (70), 2 (3), others (7)
6	RhCl ₃ hydrate	3	160	3	50	1 (40), 2 (7), others (3)
7	none		160	3	10	1 (10)
8	Rh ₆ (CO) ₁₆	5	160	63	85	1 (80), others (5)
9	none		160	63	65–70	1 (50), others (15–20) ^{c,d}
10	[{Rh(<i>μ</i> -Cl)(1,5-cod)} ₂]	10	160	16	85	1 (60), 2 (10), others (15) ^e
11	RhCl ₃ hydrate	10	160	16	85–90	1 (55), 2 (25), others (5–10) ^e

^a All reactions performed without solvent, using ca. 200–250 mg of *t*Bu₂PH·BH₃. ^b Estimated from the integrals of the ³¹P NMR spectra. However, product ratios could not always be determined to high accuracy (ca. ±5%) as small amounts of *t*Bu₂PH·BH₃ and **1** were found to sublime out of the reaction mixture at high temperatures. Also, small amounts of *t*Bu₂P(O)H (δ 67.0 ppm) and *t*Bu₂PH (δ 21.0 ppm) were sometimes detected. ^c A broad resonance at δ 28–29 ppm (unknown compound(s)) was observed. ^d A broad resonance at δ 33–34 ppm (unknown compound(s)) was observed. ^e A broad resonance at δ 8.5 ppm (unknown compound(s)) was observed.

Scheme 2

phosphinoborane [PhPH–BH₂]_{*n*}. These results indicate that there is considerable potential for the development of molecular and polymeric phosphinoborane chemistry based on metal-catalyzed dehydrocoupling procedures.

As part of our efforts to examine the scope and limitations of this novel catalytic chemistry, in this paper we report full details of our dehydrocoupling studies of the highly sterically encumbered phosphine–borane adduct *t*Bu₂PH·BH₃.

Results and Discussion

Dehydrocoupling of *t*Bu₂PH·BH₃ in the Presence of [Rh(1,5-cod)₂][OTf] or Rh₆(CO)₁₆. Similar to the formation of Ph₂PH–BH₂–Ph₂P–BH₃ from Ph₂PH·BH₃,^{12,13} the dehydrocoupling of *t*Bu₂PH·BH₃ is catalyzed by the rhodium complexes [Rh(1,5-cod)₂][OTf] or Rh₆(CO)₁₆ to give the linear dimer *t*Bu₂PH–BH₂–*t*Bu₂P–BH₃ (**1**), as is shown in Scheme 2. The results are summarized in Table 1.

[Rh(1,5-cod)₂][OTf] acts as an efficient catalyst for the dehydrogenative coupling of *t*Bu₂PH·BH₃ at 140 °C (16 h) to give compound **1** in ca. 70% yield, whereas no reaction occurred in the absence of any catalyst under these conditions (entries 1 and 2, respectively). Entries 3–7 confirm the catalytic activity of various rhodium complexes when the reaction is performed at 160 °C for 3 h: 35% of compound **1** was produced when [Rh(1,5-cod)₂][OTf] (entry 3) was used as dehydrocoupling catalyst, and 60% of compound **1** was obtained in the presence of Rh₆(CO)₁₆ (entry 4), while the control experiment without catalyst showed only 10% conversion to **1** (entry 7). Under these conditions, the chlorine-containing rhodium complexes [{Rh(*μ*-Cl)(1,5-cod)}₂] and RhCl₃ hydrate were also found to give high conversions of *t*Bu₂PH·BH₃ (entries 5 and 6, respectively), which is further discussed below. On heating *t*Bu₂PH·BH₃ to 160 °C for 63 h in the presence of Rh₆(CO)₁₆, compound **1** was obtained in 80% yield (entry 8). In the blank experiment at 160 °C (63 h) ca. 65–70% conversion of *t*Bu₂PH·BH₃ was observed; however, only 50% of compound **1** was produced together with 15–20% of other compounds (entry 9).

Pure compound **1** was obtained from a larger scale experiment following the dehydrocoupling conditions outlined in entry 8 (Table 1) and subsequent crystallization from diethyl ether. The isolated yield of the colorless, air- and moisture stable dimer **1**

was approximately 60% (based on *t*Bu₂PH·BH₃). ³¹P{¹H} NMR spectroscopy in CDCl₃ showed two broad resonances centered at δ 39.5 ppm (*t*Bu₂PH) and δ 13.2 ppm (*t*Bu₂P); the resonance at δ 39.5 ppm split further into a doublet when the proton-coupled spectrum was recorded (*J*_{PH} = 371 Hz). In the ¹H NMR spectrum, the proton attached to phosphorus was observed at δ 4.57 ppm, with a PH coupling constant of 371 Hz. The protons of the *t*Bu groups were detected as two doublets at δ 1.37 ppm and δ 1.22 ppm, respectively. The BH₃ protons appeared as a broad quartet around δ 0.45 ppm (*J*_{BH} ca. 95 Hz) while the BH₂ protons could not be observed. In the ¹¹B{¹H} NMR spectrum of **1**, only one broad multiplet in the region δ –37.2 to –40.8 ppm was detected, indicating that the two boron environments are quite similar. The ³¹P and ¹¹B NMR spectra of **1** may be compared to those of the related compound Ph₂PH–BH₂–Ph₂P–BH₃. The ³¹P{¹H} NMR chemical shifts of the latter appear at higher field and are both negative (δ –3.3 ppm, Ph₂PH, and δ –17.7 ppm, Ph₂P), which is in agreement with the relative chemical shifts observed for the free phosphines (*t*Bu₂PH, δ 21.0 ppm; Ph₂PH, δ –41.1 ppm). The ¹¹B{¹H} NMR spectrum of Ph₂PH–BH₂–Ph₂P–BH₃ displayed two distinct broad signals, one at δ –33.2 ppm (BH₂) and another at δ –37.3 ppm (BH₃). In the EI mass spectrum (70 eV) of **1** a peak at *m/z* 317 (19%) is attributable to loss of one hydrogen from the molecular ion. The 100% intensity peak corresponds to *t*Bu₂PH (*m/z* 146).

Thermal Decomposition of *t*Bu₂PH–BH₂–*t*Bu₂P–BH₃ (1**).**

A sample of pure compound **1** was heated at 175–180 °C for 16 h. The resulting off-white residue was dissolved in CDCl₃ and analyzed by ³¹P NMR spectroscopy. The complex spectrum showed major signals at δ 39.5 and 13.2 ppm (**1**), and at δ 48.9 ppm (q, *t*Bu₂PH·BH₃). Broad resonances of lower intensity found at δ 53.8, 34.0, 26.5, and 8.5 ppm are characteristic of phosphinoborane compounds; however, these species could not be identified. In addition, small amounts of *t*Bu₂P(O)H (δ 67.0 ppm) and *t*Bu₂PH (δ 21.0 ppm) were detected. Clearly, compound **1** decomposed partially upon heating with breaking of P–B bonds, since a significant amount of the starting material *t*Bu₂PH·BH₃ and traces of *t*Bu₂P(O)H and *t*Bu₂PH were formed during the reaction. Recently, Gaumont et al. reported on the flash vacuum pyrolysis of *t*Bu₂PH·BH₃ above 300 °C, and the only volatile products that could be detected by mass spectrometry were *t*Bu₂PH, BH₃ and isobutene, while the nonvolatile products were not analyzed.¹⁶

Dehydrocoupling of *t*Bu₂PH·BH₃ in the Presence of Chlorine-Containing Rhodium Complexes. A new product, *t*Bu₂PH–BH₂–*t*Bu₂P–BH₂Cl (**2**), was identified when chlorine-

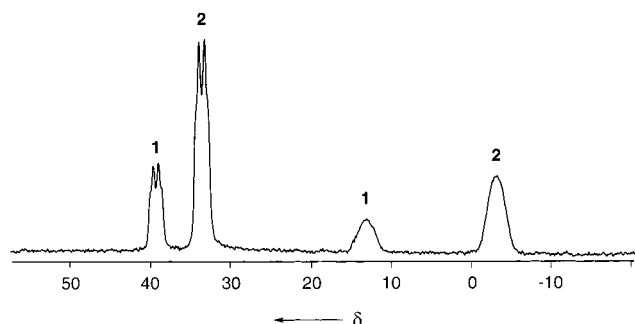


Figure 1. $^{31}\text{P}\{^1\text{H}\}$ NMR spectrum of a mixture of $t\text{Bu}_2\text{PH}-\text{BH}_2-t\text{Bu}_2\text{P}-\text{BH}_2\text{Cl}$ (**2**) and $t\text{Bu}_2\text{PH}-\text{BH}_2-t\text{Bu}_2\text{P}-\text{BH}_3$ (**1**) in CDCl_3 .

containing rhodium complexes were used to promote the dehydrocoupling of $t\text{Bu}_2\text{PH}\cdot\text{BH}_3$ (Scheme 2). Entries 5 and 6 of Table 1 demonstrate that $[\{\text{Rh}(\mu\text{-Cl})(1,5\text{-cod})\}_2]$ and RhCl_3 hydrate are suitable dehydrocoupling catalysts; however, this was accompanied by a chlorination reaction at the terminal BH_3 group of compound **1**. The amount of compound **2** could be increased using higher catalyst loads. For example, the use of $[\{\text{Rh}(\mu\text{-Cl})(1,5\text{-cod})\}_2]$ as catalyst (ca. 10 mol % Rh) gave a mixture of ca. 60% **1** and 10% **2** at 160 °C after 16 h (entry 10); however, small amounts of byproducts were also detected by ^{31}P NMR spectroscopy. A higher amount of the chlorinated product **2** (ca. 25%, along with ca. 55% **1**) was formed in the presence of RhCl_3 hydrate (ca. 10 mol % Rh) after 16 h at 160 °C (entry 11). After crystallization from diethyl ether, compound **2** was obtained as the major component (ca. 3:1 ratio, based on integration of ^1H NMR spectra). These crystals were also selected for X-ray diffraction experiments, which are discussed below. Unfortunately, compound **2** could not be isolated free of **1**. Consequently, multinuclear NMR spectroscopy of this mixture also displayed all signals characteristic for **1**. In the ^{31}P NMR spectrum, signals centered at δ 33.5 and -3.3 ppm were assigned to the $t\text{Bu}_2\text{PH}$ ($J_{\text{PH}} = 380$ Hz) and $t\text{Bu}_2\text{P}$ groups of **2**, respectively (Figure 1).

In addition, a new resonance at $\delta -15.8$ ppm in the $^{11}\text{B}\{^1\text{H}\}$ NMR spectrum was assigned to the BH_2Cl group and reflects the electron-deficient environment of the latter. The ^1H NMR resonance for the PH proton of **2** (δ 5.01 ppm, $J_{\text{PH}} = 380$ Hz) was shifted downfield by about δ 0.4 ppm from that observed for **1**, while the resonances of the $t\text{Bu}$ protons (δ 1.39 ppm and δ 1.31 ppm) were similar. BH_2 and BH_3 proton signals appeared just above the baseline, and chemical shifts could not be extracted from the ^1H NMR spectrum. The EI mass spectrum (70 eV) of this sample exhibited the molecular ion peak for **2** at m/z 352 (5%) and for **1** at m/z 318 (16%).

Discussion. Our results clearly show that the dehydrocoupling of $t\text{Bu}_2\text{PH}\cdot\text{BH}_3$ is much more sluggish than that observed for $\text{Ph}_2\text{PH}\cdot\text{BH}_3$ and requires higher temperatures. Also, it should be noted that the amount of byproducts ($t\text{Bu}_2\text{P}(\text{O})\text{H}$, $t\text{Bu}_2\text{PH}$, and compounds of unknown composition) is higher and that we did not find reaction conditions that allowed for full conversion of $t\text{Bu}_2\text{PH}\cdot\text{BH}_3$; in fact, the heating of neat compound **1** led to the starting material $t\text{Bu}_2\text{PH}\cdot\text{BH}_3$ (along with other products). This difference in ease of dehydrocoupling was also observed previously for the catalytic dehydrocoupling of $i\text{BuPH}_2\cdot\text{BH}_3$ and $\text{PhPH}_2\cdot\text{BH}_3$, where the alkyl-substituted adduct required heating at 120 °C for 13 h and the aryl-substituted adduct required only 6 h at 90–130 °C for complete conversion.^{12,13} The exact reasons for this difference in rate are not known, but it is very likely that steric problems contribute

in the case of $t\text{Bu}_2\text{PH}\cdot\text{BH}_3$. Consistent with this idea is the observation that cyclic or polymeric phosphinoboranes could not be isolated from our experiments and are obviously not a major product. Besides these steric factors, we believe that the ease of P–B bond formation also depends on the polarity of the P–H bond (and thus inductive effects). Since alkyl substituents are generally more effective donors than aryl substituents, the P–H(δ^+) bond in $t\text{Bu}_2\text{PH}$ should be less polar than that in Ph_2PH or PhPH_2 . With the hydrogens attached to boron having a partial negative charge ($\text{B}-\text{H}(\delta^-)$), the dehydrocoupling (i.e., elimination of H_2) of phosphine–borane adducts should occur at a faster rate with increasing polarity of the P–H bond.^{17,18}

Another interesting feature is the chlorination at the terminal BH_3 group of **1** to give $t\text{Bu}_2\text{PH}-\text{BH}_2-t\text{Bu}_2\text{P}-\text{BH}_2\text{Cl}$ (**2**), when the dehydrocoupling reaction is catalyzed by $[\{\text{Rh}(\mu\text{-Cl})(1,5\text{-cod})\}_2]$ or RhCl_3 hydrate. This may be a consequence of the high temperatures, causing chlorine ligand displacement from the rhodium center accompanied by chlorination at the sterically less shielded BH_3 group; this phenomenon was not observed during our studies of the catalytic dehydrocoupling of $\text{Ph}_2\text{PH}\cdot\text{BH}_3$.¹⁹ However, the chlorination of a borane fragment by a rhodium complex has been observed previously, e.g., in the reaction of $\text{BH}_3\cdot\text{THF}$ with $[\{\eta^5\text{-C}_5\text{Me}_5\}\text{RhCl}_2]_2$ to give $\text{BH}_2\text{-Cl}$.²⁰

X-ray Crystallographic Studies. The molecular structures of $t\text{Bu}_2\text{PH}\cdot\text{BH}_3$, $t\text{Bu}_2\text{PH}-\text{BH}_2-t\text{Bu}_2\text{P}-\text{BH}_3$ (**1**), and a mixture of $t\text{Bu}_2\text{PH}-\text{BH}_2-t\text{Bu}_2\text{P}-\text{BH}_2\text{Cl}$ (**2**) and **1** were determined by X-ray crystallography, and SHELXTL drawings are shown in Figures 2, 3, and 4, respectively. Crystallographic data and details of the structural determination are given in Table 2.

Crystals of $t\text{Bu}_2\text{PH}\cdot\text{BH}_3$ suitable for X-ray analysis were obtained by overnight sublimation at room temperature under an atmosphere of nitrogen. The four molecules in the unit cell are separated by the normal van der Waals distances; no intermolecular hydrogen bonding was observed. The geometry around phosphorus and boron is approximately tetrahedral, and their substituents are oriented in a staggered conformation (Figure 2). The smallest angle at phosphorus is $99.4(7)^\circ$ ($\text{H1P}-\text{P1}-\text{C5}$), and the largest is $115.45(8)^\circ$ ($\text{C1}-\text{P1}-\text{C5}$), while the angles at boron range from $105.4(12)^\circ$ to $114.9(16)^\circ$. The P–B bond length of $1.936(2)$ Å is somewhat longer than that reported for, e.g., $(\text{cHex})_2\text{PH}\cdot\text{BH}_3$ ($1.919(3)$ Å)²¹ or $\text{Ph}_3\text{P}\cdot\text{BH}_3$ (av 1.917 Å),²² but shorter than the one in $\text{RR}'\text{PH}\cdot\text{BH}_3$ (1.944 – 1.948 Å, R = mesityl, R' = menthyl) which bears organic substituents of significant size.²³

An X-ray diffraction study of **1** was carried out on a single crystal grown from diethyl ether over a period of several days

(16) Gaumont, A.-C.; Bourumeau, K.; Denis, J.-M.; Guenot, P. *J. Organomet. Chem.* **1994**, *484*, 9.

(17) The differences in dehydrocoupling rates were also confirmed by heating equimolar mixtures of $\text{Ph}_2\text{PH}\cdot\text{BH}_3$ and $t\text{Bu}_2\text{PH}\cdot\text{BH}_3$ in the presence of Rh catalysts, showing that $\text{Ph}_2\text{PH}\cdot\text{BH}_3$ reacts much faster than $t\text{Bu}_2\text{PH}\cdot\text{BH}_3$.

(18) Generally, the literature on P–B bond features is surprisingly limited and, to our knowledge, studies explaining the differences in reactivity between various phosphine–borane adducts have not been reported. For recent reviews on phosphine–borane chemistry, see: (a) Brunel, J. M.; Faure, B.; Maffei, M. *Coord. Chem. Rev.* **1998**, *178–180*, 665. (b) Carboni, B.; Monnier, L. *Tetrahedron* **1999**, *55*, 1197.

(19) A referee has pointed out that chlorination of $t\text{Bu}_2\text{PH}\cdot\text{BH}_3$ to give $t\text{Bu}_2\text{PH}-\text{BH}_2\text{Cl}$ may precede the dehydrocoupling events. We were unable to observe $t\text{Bu}_2\text{PH}-\text{BH}_2\text{Cl}$ by ^{31}P or ^{11}B NMR spectroscopy; however, it is possible that it is formed during the initial stages of the reaction and then undergoes fast dehydrocoupling with $t\text{Bu}_2\text{PH}\cdot\text{BH}_3$ to give compound **2**.

(20) Lei, X.; Shang, M.; Fehlner, T. P. *J. Am. Chem. Soc.* **1998**, *120*, 2686.

(21) Day, M. W.; Mohr, B.; Grubbs, R. H. *Acta Crystallogr.* **1996**, *C52*, 3106.

(22) Huffman, J. C.; Skupinski, W. A.; Caulton, K. G. *Cryst. Struct. Commun.* **1982**, *11*, 1435.

(23) Bader, A.; Pabel, M.; Willis, A. C.; Wild, S. B. *Inorg. Chem.* **1996**, *35*, 3874.

Table 2. Crystallographic Data and Structure Refinement

	<i>t</i> Bu ₂ PH·BH ₃	1	2 and 1
formula	C ₈ H ₂₂ BP	C ₁₆ H ₄₂ B ₂ P ₂	C ₁₆ H _{41.21} B ₂ Cl _{0.79} P ₂
fw	160.04	318.06	345.18
temp, K	150(1)	150(1)	240(1)
cryst syst	orthorhombic	triclinic	monoclinic
space group	<i>Pna</i> 2(1)	<i>P</i> 1	<i>P</i> 2(1)/ <i>n</i>
<i>a</i> , Å	15.9731(3)	8.8850(2)	8.7446(3)
<i>b</i> , Å	8.7103(4)	11.1510(4)	24.6411(9)
<i>c</i> , Å	7.8725(7)	11.3390(4)	10.4574(5)
α, deg	90	87.2910(14)	90
β, deg	90	76.9920(16)	101.857(2)
γ, deg	90	70.411(2)	90
vol, Å ³	1095.30(11)	1030.76(6)	2205.25(15)
<i>Z</i>	4	2	4
density, g cm ⁻³	0.970	1.025	1.040
abs coeff., mm ⁻¹	0.191	0.202	0.286
<i>F</i> (000)	360	356	762
cryst size, mm	0.25 × 0.20 × 0.16	0.34 × 0.28 × 0.26	0.27 × 0.25 × 0.22
θ range, deg	2.55–27.48	2.60–27.54	2.59–30.04
index ranges	−20 ≤ <i>h</i> ≤ 20, −11 ≤ <i>k</i> ≤ 11, −10 ≤ <i>l</i> ≤ 10	0 ≤ <i>h</i> ≤ 11, −13 ≤ <i>k</i> ≤ 14, −14 ≤ <i>l</i> ≤ 14	−9 ≤ <i>h</i> ≤ 12, −34 ≤ <i>k</i> ≤ 0, −10 ≤ <i>l</i> ≤ 14
reflns collected	6569	11323	16496
indep reflns	2344	4705	6348
	(<i>R</i> _{int} = 0.043)	(<i>R</i> _{int} = 0.040)	(<i>R</i> _{int} = 0.028)
GOF on <i>F</i> ²	1.023	1.055	1.035
<i>R</i> 1 ^a (<i>I</i> > 2σ(<i>I</i>))	0.0350	0.0396	0.0535
w <i>R</i> 2 ^b (all data)	0.0821	0.0975	0.1381
peak/hole, e Å ⁻³	0.156/−0.193	0.267/−0.315	0.365/−0.282

^a $R1 = \sum ||F_o| - |F_c|| / \sum |F_o|$. ^b $wR2 = \{ \sum [w(F_o^2 - F_c^2)^2] / \sum [w(F_o^2)^2] \}^{1/2}$.

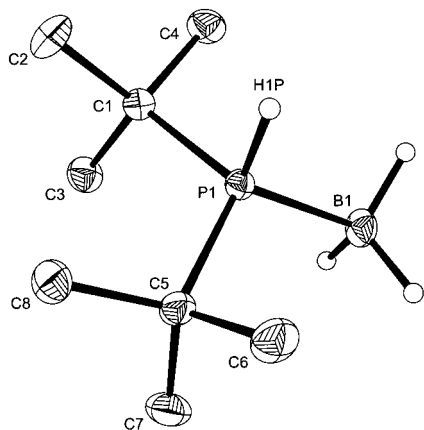


Figure 2. Molecular structure of *t*Bu₂PH·BH₃. Selected bond lengths (Å) and angles (deg): P1–B1 1.936(2), P1–C1 1.8568(18), P1–C5 1.8627(18), P1–H1P 1.350(16); H1P–P1–B1 113.4(7), C1–P1–B1 113.03(10), C5–P1–B1 112.76(10). Hydrogen atoms attached to carbon atoms are omitted.

at room temperature. Compound **1** crystallizes in the triclinic space group *P*1̄. The molecular structure of **1** (Figure 3) is very similar to that of Ph₂PH–BH₂–Ph₂P–BH₃.^{12,13} The internal P1–B1 bond length is 1.9794(18) Å, while the terminal P–B distances are slightly shorter (P2–B1 1.9544(19) Å, P1–B2 1.9536(19) Å). This pattern of short–long–short P–B distances was also observed in Ph₂PH–BH₂–Ph₂P–BH₃ (P2–B1 1.923(2) Å, P1–B1 1.944(2) Å, P1–B2 1.932(2) Å), as well as for the two P–B bonds closest to the P terminus in Ph₂PCl–BH₂–Ph₂P–BH₂Cl (1.907(6), 1.959(6), 1.953(6) Å);²⁴ however, the overall values are larger in compound **1**. Also, the P–B bonds in **1** are significantly longer than in the starting material *t*Bu₂PH·BH₃ (1.936(2) Å). The bond angles around P1 (105.89(7)–116.39(8)°) and P2 (101.4(6)–114.39(7)°), as well as B1 (105.3(9)–114.36(9)°) and B2 (104.9(10)–115.2(14)°), deviate quite significantly from the tetrahedral value of 109.5°. The

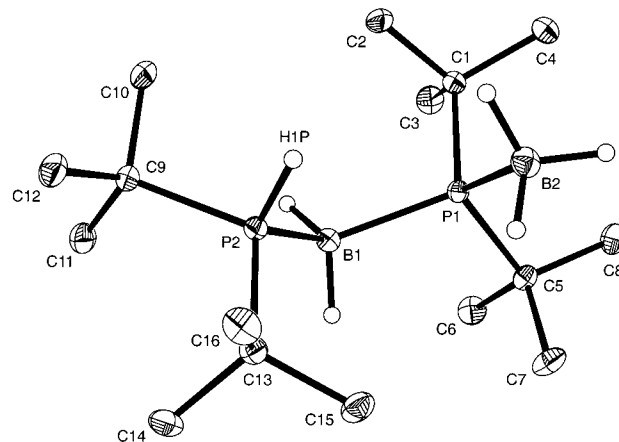


Figure 3. Molecular structure of *t*Bu₂PH–BH₂–*t*Bu₂P–BH₃ (**1**). Selected bond lengths (Å) and angles (deg): P2–B1 1.9544(19), P1–B1 1.9794(18), P1–B2 1.9536(19), P2–H1P 1.303(15), P1–C1 1.8881(15), P1–C5 1.8882(16), P2–C9 1.8718(15), P2–C13 1.8805(15); P2–B1–P1 114.36(9), B2–P1–B1 116.39(8), H1P–P2–B1 113.1(7). Hydrogen atoms attached to carbon atoms are omitted.

conformation adopted by **1** has a torsion angle of 14.41(13)° in the P–B–P–B chain, which minimizes the steric interactions between the *t*Bu groups attached to P1 and P2, respectively. For comparison, the torsion angle in Ph₂PH–BH₂–Ph₂P–BH₃ is 39.35(17)°, and it is ca. 60° in Ph₂PCl–BH₂–Ph₂P–BH₂Cl.²⁴ Furthermore, the P–C distances in **1** (av P–C(*t*Bu) 1.8822(16) Å) are longer than those found in Ph₂PH–BH₂–Ph₂P–BH₃ (av P–C(Ph) 1.812(2) Å). The sterically highly encumbered phosphorus centers and carbon hybridization effects are the most likely explanation for the long P–B and P–C distances in **1**, respectively.

Single crystals of a mixture of compounds **2** and **1** were grown from a diethyl ether solution at room temperature. The crystal was monoclinic with space group *P*(2)₁/*n*. The final refinement of the site occupancy factors proceeded to give 0.79 for BH₂Cl (compound **2**) and 0.21 for BH₃ (compound **1**). This ratio is in good agreement with the integration ratio of the ¹H NMR spectra, as discussed above. The molecular structure is

(24) Greenwood, N. N.; Kennedy, J. D.; McDonald, W. S. *J. Chem. Soc., Dalton Trans.* **1978**, 40.

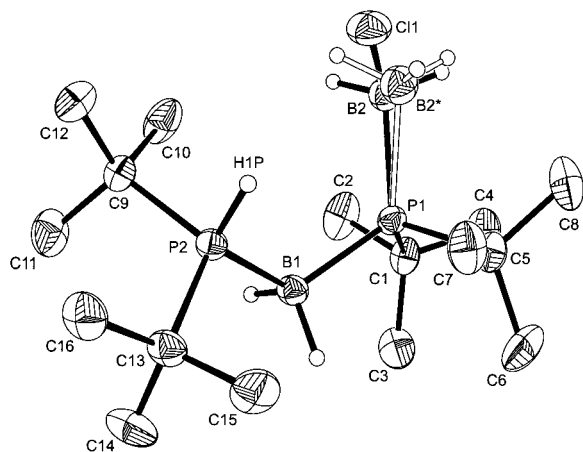


Figure 4. Molecular structure of the mixture of *t*Bu₂PH-BH₂-*t*Bu₂P-BH₂Cl (**2**) and *t*Bu₂PH-BH₂-*t*Bu₂P-BH₃ (**1**). Selected bond lengths (Å) and angles (deg): P2-B1 1.954(2), P1-B1 1.967(2), P1-B2 1.955(3), P2-H1P 1.305(19), B2-C11 1.898(4); P2-B1-P1 119.23(11), B2-P1-B1 120.98(11), H1P-P2-B1 115.2(8), P1-B2-C11 110.32(16). Hydrogen atoms attached to carbon atoms are omitted.

shown in Figure 4. It is the least precise of those reported here, and only the major component **2** is discussed.

The terminal bond lengths P2-B1 (1.954(2) Å) and P1-B2 (1.955(3) Å) are comparable to those observed in **1**, while the internal bond length P1-B1 (1.967(2) Å) is slightly shorter. The phosphorus and boron environments in **2** also exhibit distortion from the ideal tetrahedral geometry (P1, 102.42(13)–120.98(11)°; P2, 101.4(8)–115.2(8)°; B1, 103.4(10)–119.23(11)°); the P1-B2-C11 angle is 110.32(16)°. The B-Cl bond in **2** of 1.898(4) Å is somewhat longer than that reported for the related four-membered chain Ph₂PCl-BH₂-Ph₂P-BH₂Cl (B-Cl 1.877(7) Å).²⁴

Summary

With the synthesis of *t*Bu₂PH-BH₂-*t*Bu₂P-BH₃ (**1**) and *t*Bu₂PH-BH₂-*t*Bu₂P-BH₂Cl (**2**) we have demonstrated again the usefulness of rhodium complexes in the catalytic formation of phosphorus-boron bonds. In contrast to the catalytic dehydrocoupling of Ph₂PH·BH₃, *t*Bu₂PH·BH₃ reacts much slower and does not yield appreciable amounts of cyclic species. This may primarily be due to the high steric requirements of the *t*Bu₂ groups but may also be attributed to the low polarity of the P-H bond in *t*Bu₂PH·BH₃.

Experimental Section

General Information. All reactions were performed under an atmosphere of dry nitrogen while workup procedures were carried out in air. *t*Bu₂PH, [Rh(1,5-cod)₂][OTf], Rh₆(CO)₁₆ (Strem), and RhCl₃ hydrate (Pressure Chemical Co.) were purchased and used as received. [Rh(μ-Cl)(1,5-cod)₂]₂ was prepared following a literature procedure.²⁵ *t*Bu₂PH·BH₃ was prepared following a procedure analogous to that for *i*BuPh₂·BH₃.¹³ NMR spectra were recorded on a Varian Gemini or Mercury 300 MHz spectrometer. Chemical shifts are referenced to solvent peaks (¹H) or external BF₃·Et₂O (¹¹B) or H₃PO₄ (³¹P). Mass spectra were obtained with a VG 70-250S mass spectrometer operating in electron impact (EI) mode. Elemental analyses were performed by Quantitative Technologies, Inc., Whitehouse, NJ.

X-ray Structural Characterization. Crystal data and details of the data collection are provided in Table 2. Diffraction data were collected on a Nonius Kappa-CCD using graphite-monochromated Mo Kα radiation (λ = 0.71073 Å). A combination of 1° φ and ω (with κ offsets) scans were used collect sufficient data. The structures were solved and

refined with the SHELXTL-PC V5.1 software package.²⁶ The data frames were integrated and scaled using the Denzo-SMN package.²⁷ Refinement was by full-matrix least squares on F² using all data (negative intensities included). Molecular structures are presented with ellipsoids at a 30% probability level. In all structures hydrogens bonded to carbon atoms were included in calculated positions and treated as riding atoms. Hydrogens attached to boron and phosphorus atoms were refined with isotropic thermal parameters, except for hydrogens attached to B2 in the mixture of compounds **2** and **1**, which were also included in calculated positions. Crystallographic data were deposited in the Cambridge Crystallographic Data Centre with codes CCDC-166925 (*t*Bu₂PH·BH₃), CCDC-166926 (**1**), and CCDC-166927 (**2** and **1**).

***t*Bu₂PH-BH₂-*t*Bu₂P-BH₃ (**1**).** Neat *t*Bu₂PH·BH₃ (0.84 g, 5.25 mmol) and Rh₆(CO)₁₆ (ca. 20 mg, 2 mol % Rh) were stirred at 160 °C for 63 h (Table 1, entry 8). The dark brown reaction mixture became liquid upon heating and solidified when cooled to room temperature. Recrystallization from diethyl ether gave colorless crystals of **1** which were suitable for single-crystal X-ray analysis. Isolated yield: 0.50 g (60%). Mp: 130–131 °C. ¹H NMR (300 MHz, CDCl₃): δ = 4.57 (dm, J_{PH} = 371 Hz, PH), 1.37 (d, J_{PH} = 14.0 Hz, *t*Bu), 1.22 (d, J_{PH} = 11.8 Hz, *t*Bu), 1.10 to -0.10 (br q, J_{BH} ca. 95 Hz, BH₃), BH₂ not observed. ¹¹B{¹H} NMR (96 MHz, CDCl₃): δ = -37.2 to -40.8 (br m, BH₂ and BH₃). ³¹P{¹H} NMR (121 MHz, CDCl₃): δ = 39.5 (br, *t*Bu₂PH), 13.2 (br, *t*Bu₂P). MS (EI, 70 eV): *m/z* (%) 317 (19) [M⁺ - H], 304 (35) [M⁺ - BH₃], 146 (100) *t*Bu₂PH. Anal. Calcd for C₁₆H₄₂B₂P₂: C, 60.4; H, 13.3. Found: C, 59.7; H, 12.8.

Thermal Decomposition of *t*Bu₂PH-BH₂-*t*Bu₂P-BH₃ (1**).** A sample of **1** (0.10 g) was loaded into a sublimator and heated and maintained at 175–180 °C for 16 h. A small amount of a colorless sublimate was noted on the coldfinger and was subsequently identified as *t*Bu₂P(O)H (³¹P NMR). The off-white residue in the sublimator was analyzed by ³¹P NMR spectroscopy without further purification. ³¹P-{¹H} NMR (121 MHz, CDCl₃): δ = 67.0 (s, *t*Bu₂P(O)H), 53.8 (br), 48.9 (q, *t*Bu₂PH·BH₃), 39.5 (br, *t*Bu₂PH, **1**), 34.0 (br), 26.5 (br), 21.0 (s, *t*Bu₂PH), 13.2 (br, *t*Bu₂P, **1**), 8.5 (br).

***t*Bu₂PH-BH₂-*t*Bu₂P-BH₂Cl (**2**) and *t*Bu₂PH-BH₂-*t*Bu₂P-BH₃ (**1**).** Neat *t*Bu₂PH·BH₃ (0.27 g, 1.69 mmol) and RhCl₃ hydrate (ca. 45 mg, 10 mol % Rh) were stirred at 160 °C for 16 h (Table 1, entry 11). After cooling to room temperature the dark brown reaction mixture was recrystallized from diethyl ether to give colorless crystals of a mixture of compounds **2** and **1** which were suitable for single-crystal X-ray analysis. Isolated yield 0.18 g. These compounds could not be separated by fractional crystallization and could not be distinguished by their crystal habits. ¹H NMR (300 MHz, CDCl₃): δ = 5.01 (dm, J_{PH} = 380 Hz, PH, **2**), 4.56 (dm, J_{PH} = 371 Hz, PH, **1**), 1.39 (d, J_{PH} = 14.0 Hz, *t*Bu, **2**), 1.37 (d, J_{PH} = 14.0 Hz, *t*Bu, **1**), 1.31 (d, J_{PH} = 12.1 Hz, *t*Bu, **2**), 1.22 (d, J_{PH} = 11.8 Hz, *t*Bu, **1**), 1.10 to -0.10 (br q, J_{BH} ca. 95 Hz, BH₃), BH₂ not observed. ¹¹B{¹H} NMR (96 MHz, CDCl₃): δ = -15.8 (br, BH₂Cl, **2**), -36.0 to -41.5 (br m, BH₂ and BH₃, **2** and **1**). ³¹P{¹H} NMR (121 MHz, CDCl₃): δ = 39.3 (br, *t*Bu₂PH, **1**), 33.5 (br, *t*Bu₂PH, **2**), 13.0 (br, *t*Bu₂P, **1**), -3.3 (br, *t*Bu₂P, **2**). MS (EI, 70 eV): *m/z* (%) 352 (5) [M⁺(**2**)], 318 (16) [M⁺(**1**)], 57 (100) *t*Bu.

Acknowledgment. This research was supported by the Natural Science and Engineering Research Council of Canada (NSERC), and the Petroleum Research Fund (PRF) administered by the American Chemical Society (ACS). H.D. thanks the Deutsche Forschungsgemeinschaft (DFG) for a postdoctoral fellowship.

Supporting Information Available: Figures giving ¹H and ³¹P-{¹H} NMR spectra of compound **1**. Crystallographic data in CIF format. This material is available free of charge via the Internet at <http://pubs.acs.org>.

IC0100626

(26) Sheldrick, G. M. *SHELXTL-PC*, V5.1; Bruker Analytical X-ray Systems Inc.: Madison, 1997.

(27) Otwinowski, Z.; Minor, W. *Methods Enzymol.* **1997**, *276*, 307.

(25) Giordano, G.; Crabtree, R. H. *Inorg. Synth.* **1979**, *19*, 218.